

Supporting information

‘Nano on Micro’ Hierarchical Porous All Carbon Structures: An Insight into the Interfacial Interactions with Bacteria

Shriram Janghela,^a Nagendra Singh Neeraj,^a Neha Agarwal,^{a,b} Kavita Agarwal,^c Debmalya Roy^{a*}, Kingsuk Mukhopadhyay^c and Namburi Eswara Prasad^c

^aDirectorate of Nanomaterials and Technologies, DMSRDE, GT Road, Kanpur, India-208013

^bDIPAS, Lucknow Road, Timarpur, Delhi, India- 110054

^cDMSRDE, GT Road, Kanpur, India-208013.

INDION® 225 H
Hydrochloric acid Regeneration

<p>Description</p> <p>INDION 225 H is a premium grade strong acid cation exchange resin containing sulphonic acid groups. It is based on cross-linked polystyrene and has a gel structure. The resin has high capacity and excellent kinetics.</p>	<p>Applications</p> <p>De-ionising</p> <p>INDION 225 H in hydrogen form is used as a first step in de-ionising. Technical data for co-flow and counter current regeneration is given in this literature.</p>
---	--

Characteristics

Appearance	:	Golden yellow to brown beads
Matrix	:	Styrene divinylbenzene copolymer
Functional Group	:	Sulphonic acid
Ionic form as supplied	:	Hydrogen, H ⁺
Total exchange capacity	:	1.8 meq/ml, minimum
Moisture holding capacity	:	49 -55 %
Shipping weight *	:	780 kg/m ³ approximately
Particle size range	:	0.3 to 1.2 mm
> 1.2 mm	:	5.0%, maximum
< 0.3 mm	:	1.0%, maximum
Uniformity co-efficient	:	1.7, maximum
Effective size	:	0.45 to 0.55 mm
Maximum operating temperature	:	120°C
Operating pH range	:	0 to 14
Volume change	:	Na to H, 8 % approximately
Resistance to reducing agents	:	Good
Resistance to oxidizing agents	:	Generally good, chlorine should be absent

* Weight of resin, as supplied, occupying 1 m³ in a unit after backwashing & draining.

Fig S1: The data sheet of Indion 225 H resin beads purchased from INDION, Gujrat, India.

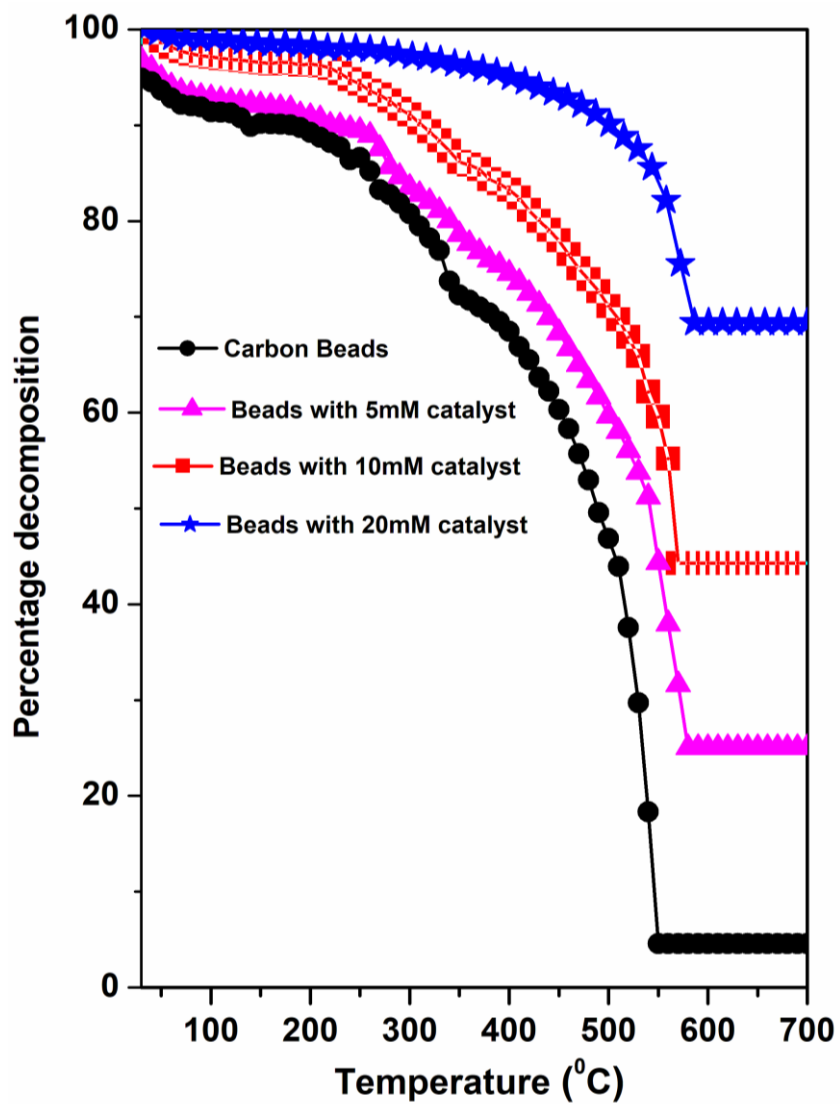


Fig S2: The TGA thermographs in air of carbon beads (black dots) and beads soaked into $\text{Fe}(\text{C}_5\text{H}_7\text{O}_2)_3$ of 05 (magenta triangles), 10 (red squares) and 20 (blue stars) mM concentrations.

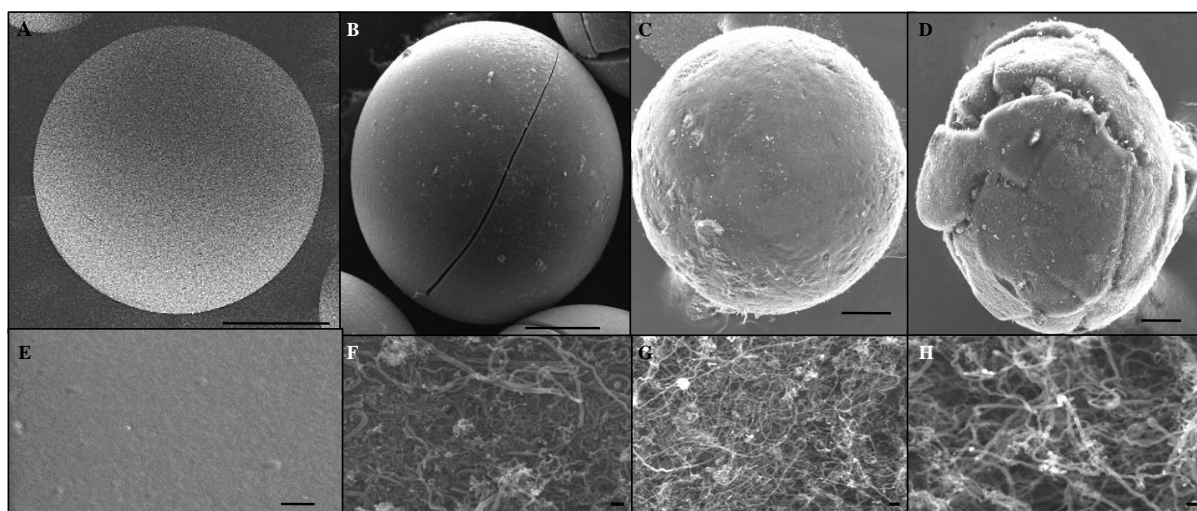


Fig S3: SEM images of carbon bead surface before (A&E) and after nanofibers growth process in CCVD using 05 (B&F), 10 (C&G) and 20 (D&H) mM concentration of catalyst precursor $\text{Fe}(\text{C}_5\text{H}_7\text{O}_2)_3$ in ethanol. The scale bars of SEM are 200 μm (A), 100 μm (B-D), 1 μm (E) and 100 nm (F-H) respectively. The yield of nanofibers are less than 10 weight percentage of carbon bead mass in all the cases which were determined by thermogravimetric analysis in inert atmosphere.

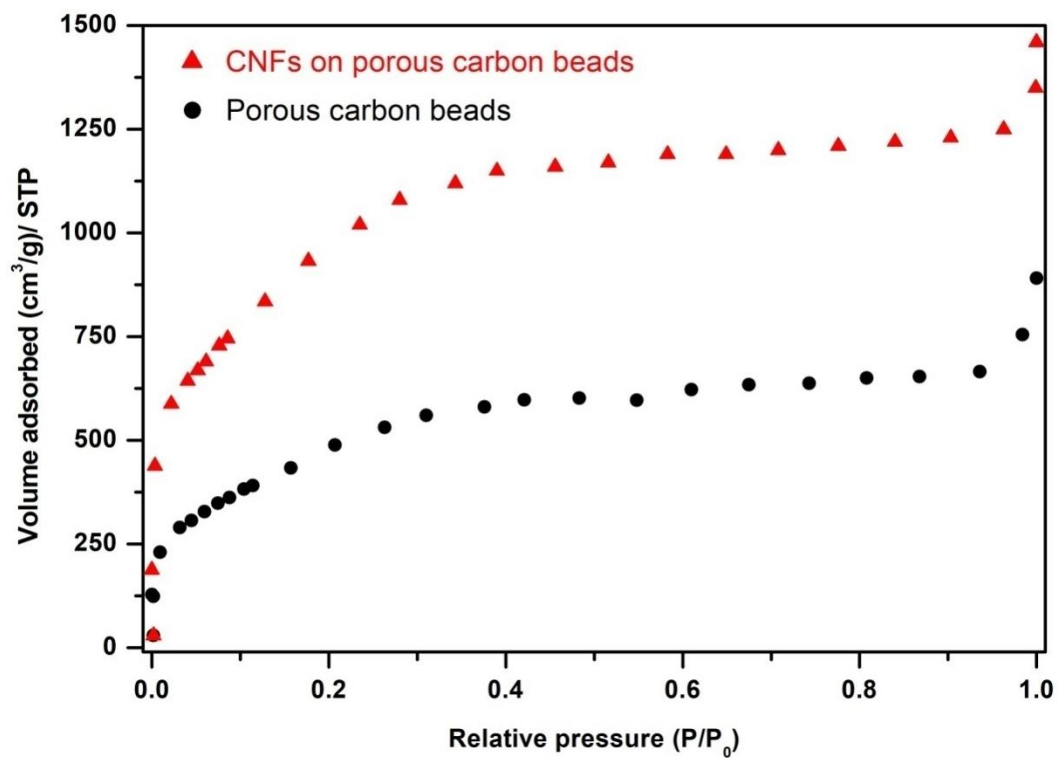


Fig S4: Nitrogen adsorption isotherms for the degassed porous carbon bead (black circles) and carbon nanofibers mat on porous carbon beads (red triangles) using Quantachrome Autosorb-1-C BET Surface Area & Pore Volume Analyzer.

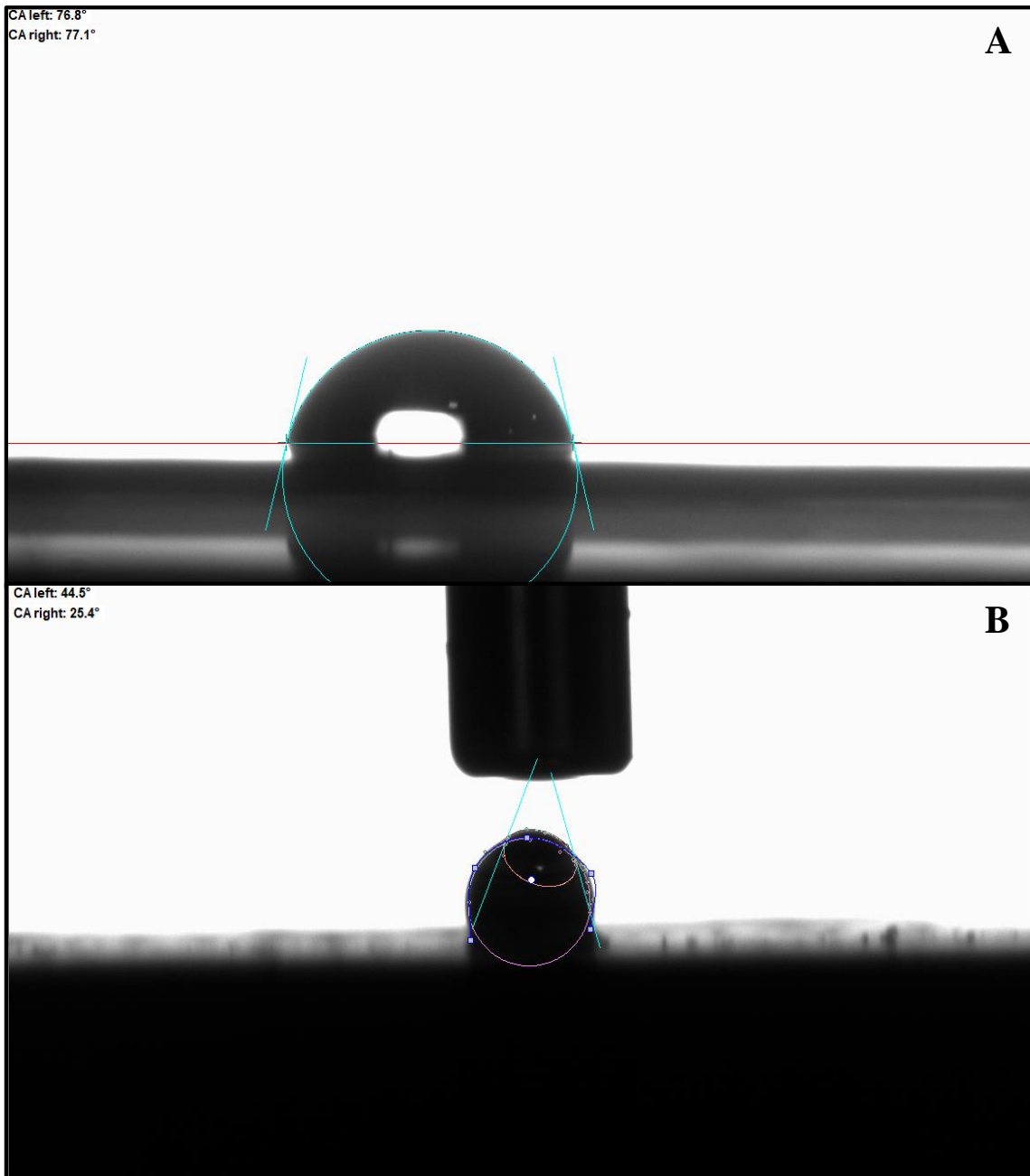


Fig S5: The contact angle measurement by sessile drop mode of bare porous carbon bead (A) and brush heap structures on carbon spheres (B) where the contact angle is 76.8 and 44.6 respectively.

Sample	Zone of inhibition (ZOI) mm	Minimal inhibitory concentration (MIC) PPM
Carbon beads (5mg/L)	8.2±0.3	120±0.6
Carbon beads (10mg/L)	8.8±0.4	
Carbon beads (30mg/L)	9.3±0.6	
Carbon beads with carbon nanofibrous hairs (5mg/L)	11.9±0.5	84±0.9
Carbon beads with carbon nanofibrous hairs (10mg/L)	12.7±0.8	
Carbon beads with carbon nanofibrous hairs (30mg/L)	13.1±0.9	

TableT1: Zone of inhibition (ZOI) and minimum inhibitory concentration (MIC) of the porous carbon beads with and without nanofibrous hairs against gram negative bacteria at 5,10 and 30 ppm level. The experiments were performed in triplicate sets and the values are presented as mean ± standard deviation.

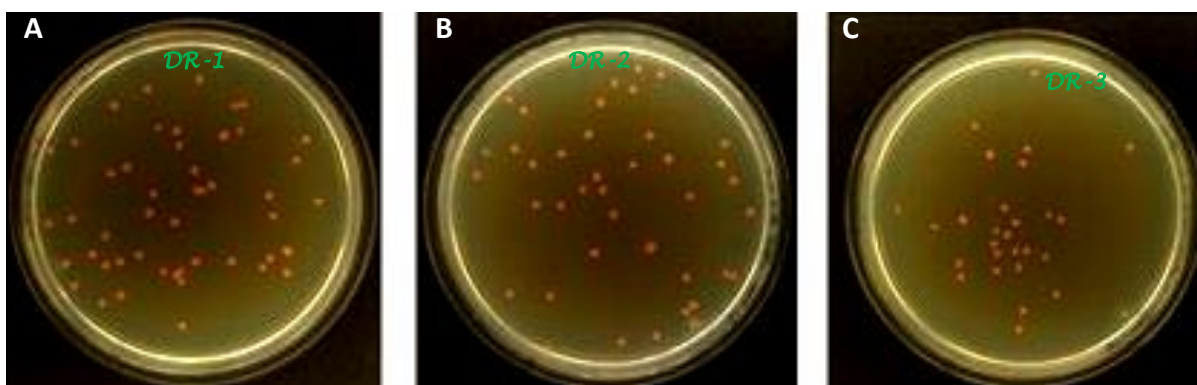


Fig S6: The images of agar plate culture for counting colony forming units where (A), (B) and (C) represent bacterial colony in presence of pristine bead, beads embedded with iron nanoparticles and beads with nanofibers respectively.

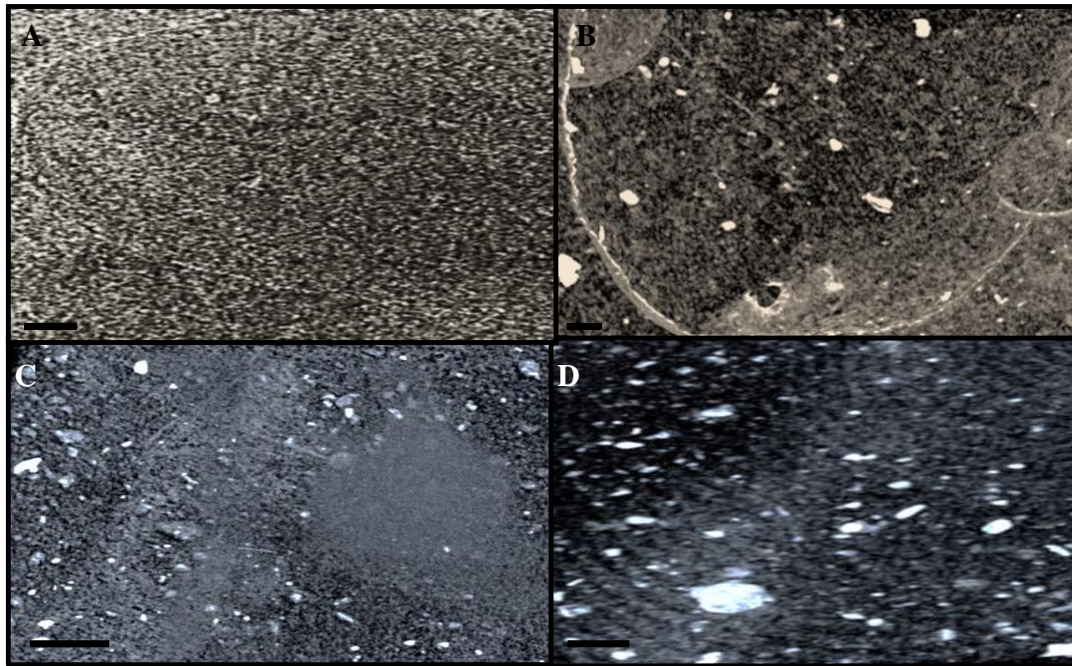


Fig S7: The optical transmission images (low resolution A-B and high magnification C-D) of the surface of the carbon beads after the antibacterial studies at 10^7 cfu mL⁻¹ where (A, C) represents bare carbon bead surface and (B, D) illustrates the carbon nanofiberous web on the porous carbon bead surface where the scale bars are 10 μ m.

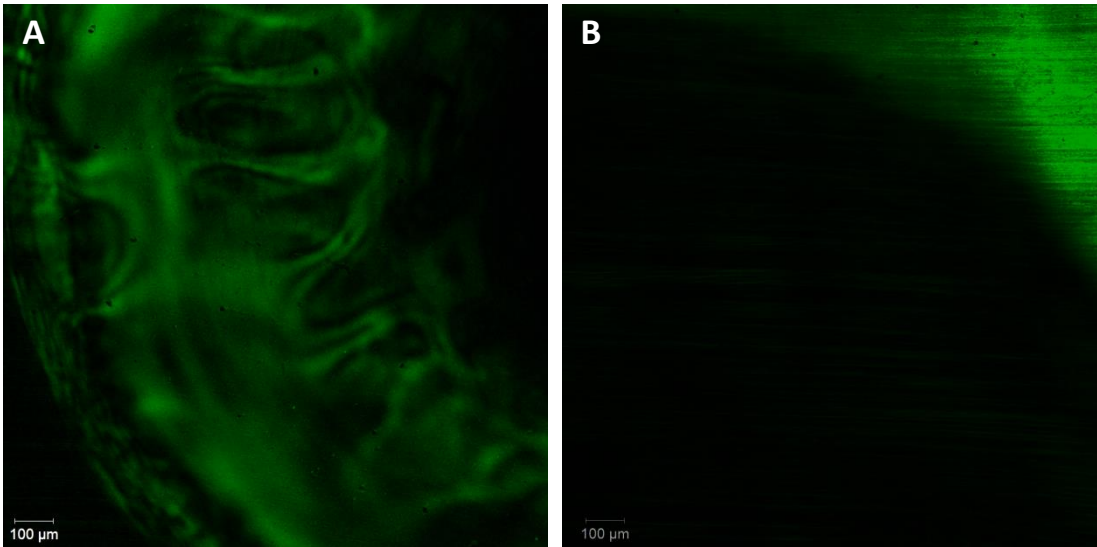


Fig S8: The figures A and B represent the fluorescent images of the biofilm formed on the nanofibers mat by the immobilized bacteria on the carbon bead and the same after incubation for 2 minutes in PBS buffer respectively.

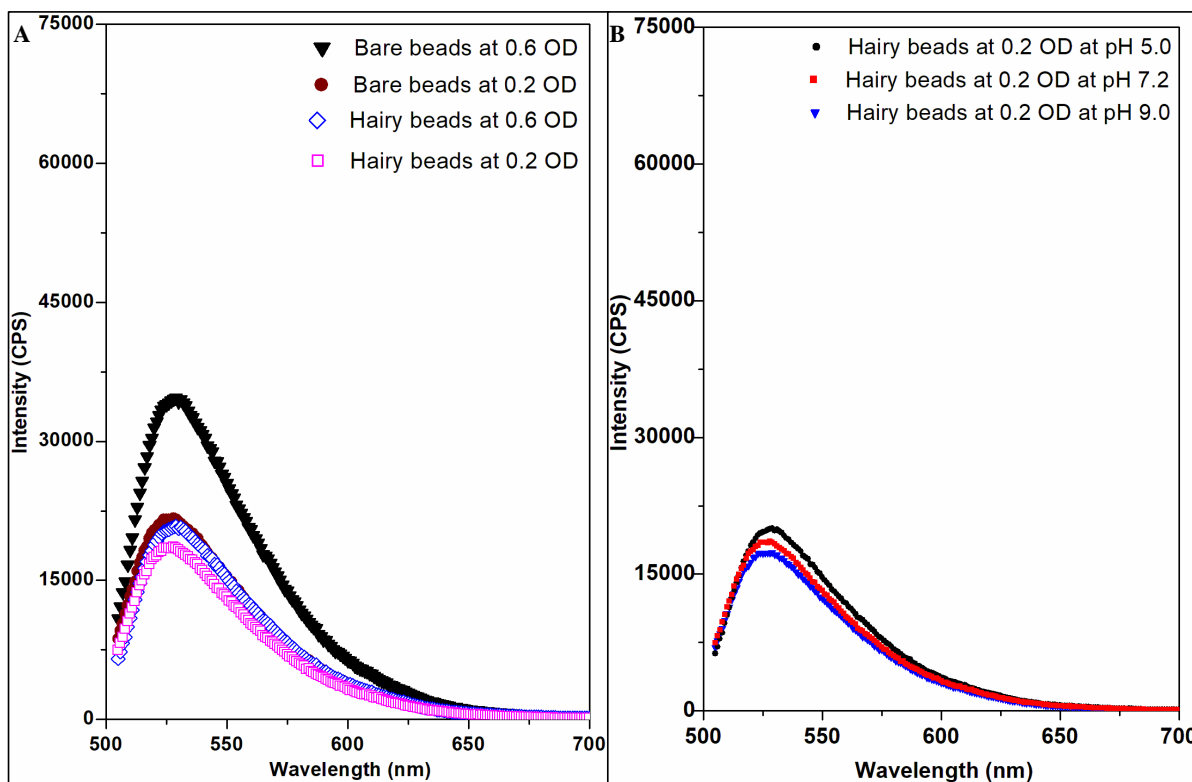


Fig S9: In order to obtain the fluorescence intensity of unbound E.Coli bacteria, the supernatant of the acridine stained beads with and without CNFs were centrifuged at centrifuged at 8000 rpm for 5 min. The supernatant of the solution was discarded and the obtained cell pellet was washed with 1x PBS buffer (pH 7.2) to completely remove the traces of unbound acridine dye. The stained E.Coli cells were again dispersed in PBS buffer and measured the fluorescence intensity. The florescent spectra intensities of 0.6 and 0.2 OD concentrations of bacterial colonies from bare carbon beads and CNFs on carbon beads are compiled in figure A. To further understand the effect of pH on the unbound bacteria, the pH solution of the acridine stained beads were modified to 5.0, 7.2 and 9.0. The figure B represents the florescent spectra intensities of 0.2 OD concentrations of bacterial colony from hairy carbon beads at different pH.

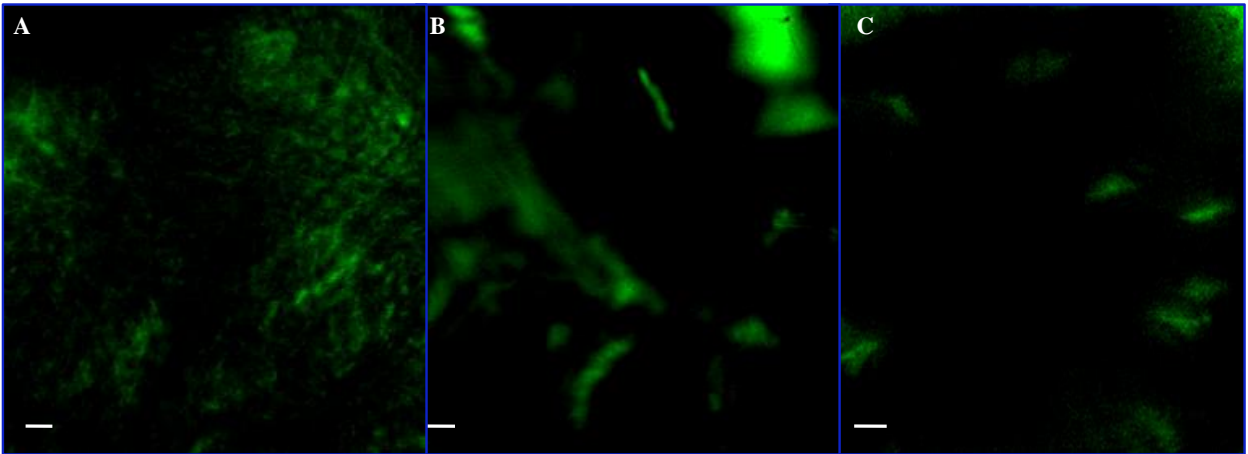


Fig S10: The florescent images of stained bacteria impregnated beads by acridine orange after spinning in a buffer solution of pH= 9.0 for 02 min, 1000 rpm (A), 10 min, 2000 rpm (B), 20 min, 3000 rpm (C) respectively. The scale bar of florescent image is 100 μ m.